IUG Journal of Natural and Engineering Studies
Vol.20, No.2, pp 1-14 **2012**, ISSN 1726-6807, http://www.iugaza.edu.ps/ar/periodical/

Investigation of the effect of different dyes on organic light emitting diode properties

Hussam S. Musleh[a], Taher M. El-Agez[a], Ahmed A. El Tayyan[b], and Sofyan A. Taya[a*]
[a]Physics Department, Islamic University of Gaza, Gaza, Palestine
[b]Physics Department, Al Azhar University, Gaza, Palestine
*Corresponding Author: Sofyan A. Taya,
Email: staya@iugaza.edu.ps

Abstract: In this article we report electroluminescence (EL) from double and single layer thin film devices comprising poly(N-vinylcarbazole) (PVK) films doped with various new emitter molecules (dyes). The structure of the single layer device is doped PVK sandwiched between indium tin oxide (ITO) and aluminum (Al) layers as anode and cathode, respectively. We have used 2% concentration of Rhodamine 6G, carbocyanine, 1,2,4 oxadiazole, and fluroscein dyes. The double layer device has the structure ITO/PVK/8-hydroxyquinoline aluminum (Alq_3)/Al. We have studied the IV characteristics as well as the variations of the EL with voltage and current of these devices.

Keywords: Organic light emitting diode, PVK, electroluminescence, IV characteristics

دراسة تأثير الأصباغ المختلفة على خصائص الثنائيات العضوية الباعثة للضوء

الملخص: ندرس في هذا العمل الانبعاث الضوئي من أفلام رقيقة مكونة من طبقة واحدة ومن طبقتين تحتوي على المادة العضوية poly(9-vinylcarbazole) (PVK) المطعمة بأصباغ مختلفة. الأفلام ذات الطبقة الواحدة تشكلت من مادة PVK المطعمة بين طبقتين من ITO و Al كقطبين. الأصباغ التي استخدمت هي carbocyanine, 1,2,4 oxadiazole, Rhodamine 6G, fluroscein. الأفلام ذات الطبقتين احتوت على طبقة إضافية من مادة Alq_3 . قمنا بدراسة تفصيلية لمنحنيات التيار والجهد والانبعاثية الضوئية مع كل من الجهد والتيار.

1. Introduction

Thin organic films have many attractive features and are being widely investigated by researchers for use in electronic devices [1-7]. The main advantage of organic materials over inorganic semiconductors is that they can be deposited by evaporation, spin-coating, screen printing, and casting. These deposition methods are simpler and cheaper than most of the deposition methods used in inorganic semiconductors.

Organic light emitting diodes (OLEDs) have been studied intensively since C. Tang and S. VanSlyka [1] reported their double layer organic light emitting device. In 1990, Burroughes et al. [2] made another important

discovery when they detected electroluminescence (EL) from devices based on luminescent conjugated polymers. Much progress has been achieved and the device performance has improved dramatically since then. One of the advantages of an OLED display over the traditional liquid crystal display is that OLEDs do not require a backlight to function. This means that OLEDs draw far less power. Also, OLED displays have a wide viewing angle.

An OLED generally consists of a single or multiple layers sandwiched between transparent indium tin oxide (ITO) anode and a metal cathode. By applying a positive bias to the anode and a negative bias to the cathode, both holes and electrons can be injected into the thin organic layer (layers). When an electron and a hole meet they form a bound state, an exciton, inside the emissive layer. Then, the exciton's electron and hole may recombine, producing EL. Many organic and organo-metallic compounds have been tested as emitters in organic light emitting diodes [8-11].

PVK is a well known polymer with interesting properties. Its excellent electrical properties combined with its chemical and thermal resistance make it useful in the electronics industry. It is used commercially as a mica substitute, and as a paper-capacitor impregnant. Because of the unique PVK photoconductivity and photorefractivity characteristics, there is a renewed interest in PVK for holography, nonlinear optics, electronic data storage, electro-optics, and EL [12–15].

In this paper, we report EL from five OLED samples. One of these samples consists of a double layer with the structure ITO/PVK/8-hydroxyquinoline aluminum (Alq_3)/Al. The other OLEDs are single layer type in which PVK is doped with the rhodamine 6G, carbocyanine, 1,2,4 oxadiazole and fluroscein dyes. These samples are listed in table (1). The structute of PVK, rhodamine 6G, carbocyanine, 1,2,4 oxadiazole, fluroscein, and Alq_3 is shown in Fig. 1.

2. Experimental work

ITO coated glass substrates purchased from delta technologies, USA with sheet resistance of 8–12 Ω/□ were cut carefully into pieces of 2.5 cm × 2.5 cm. Each sample was arranged in an 4 × 4 array of devices. The active area of each device was 2.2 mm × 2.2 mm. The ITO plates were cleaned thoroughly by wiping each electrode surface by a cotton pad wetted with acetone. Then, an electric tape was stuck at the conductive side of the ITO coated glass substrate. The ITO electrodes were then etched to form the desired pattern by immersing them in Aqua-Regia acid (solution of 20% HCl and 5% HNO_3) for 15 minutes at 60°C. The electrodes were cleaned using Xyelen, then rinsed in deionized water to remove away the leftover acids on their surfaces. Upon completing the etching process, they were

cleaned using DC argon plasma for 8 minutes. Then, the electrodes were left inside an oven at 80°C over night.

To prepare the single film samples, an amount of 30 mg of PVK (Sigma-Aldrich, USA) was dissolved in 15 ml of chloroform. An amount of 2 % by weight of the dopant (rhodamine 6G, carbocyanine, 1,2,4 oxadiazole and fluroscein dyes) was added to the solution. The solution was then stirred thoroughly and filtered. Few drops of the blend solution were spun at 1750 rpm for one minute to form thin film on the etched ITO. For the double layer sample, the Alq_3 layer was deposited on the PVK film using thermal vacuum evaporation at 1.7×10^{-5} torr in low rate deposition condition for one minute. The samples were kept under vacuum at 80°C for 24 hours to remove residual solvents inside the polymer layer. The Al cathode was deposited thermally under vacuum condition (10^{-5} torr) at a low deposition rate on the top of the structure through a five fingers shadow mask. Finally, wires were connected to the electrodes using silver glue. The structure of the single and double film devices is shown in Fig. 2.

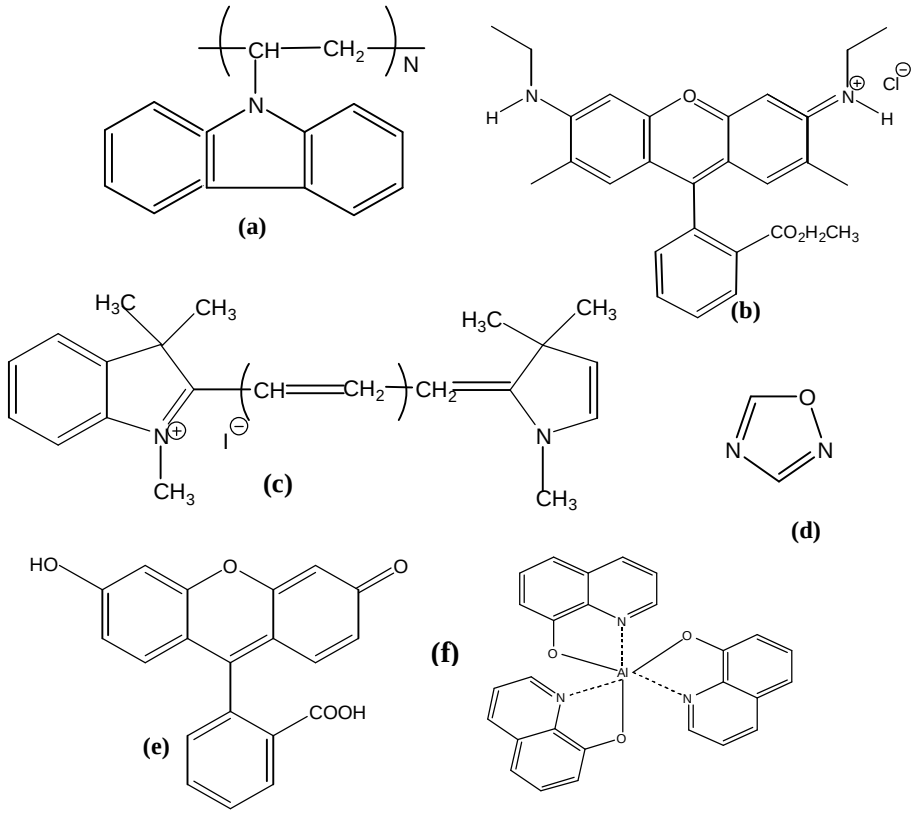

Fig. 1. The structures of (a) PVK, (b) Rhodamine 6G, (c) Carbocyanine, (d) 1,2,4 oxadiazole, (e) fluroscein, and (f) Alq_3.

Figure 3 shows a schematic diagram of the experimental setup. The relative light intensity was measured using a photomultiplier tube (PMT).
The data were recorded and saved as an ASCII file, then, analyzed and plotted. Electrical measurements were conducted at room temperature and in nitrogen chamber in order to prevent oxidation to increase the device life time. The driving voltages and the currents were obtained and measured using a MetraByte's Das-20 data acquisition card interfaced with a personal computer. The output of the PMT was amplified then collected by the same data acquisition card.

3. Results and Discussion

PVK is a well known hole transporting polymer that exhibits essentially trap-free transport for holes [15]. Accordingly, the injected holes can reach the Al electrode without recombination, unless they encounter electrons injected from the Al electrode.
As mentioned in the experimental work section, five samples (S_1 through S_5) have been prepared. The structures of these samples are given in table 1. Figure 4 illustrates the I-V characteristics for all samples. It is clear from the figure that the current increases exponentially with the applied voltage.
The threshold voltage, V_T, is an important parameter characterizing the operation of an OLED. In general it is the voltage at which an OLED starts to emit light. The current increases sharply when the applied voltage exceeds V_T. The threshold voltages were estimated by linearly extrapolating the linear rise of I-V curves back to the voltage axis [16,17]. Estimated values of V_T for each sample is given in Table (1).
The IV characteristics in Fig. 4 indicate a large leakage current, which is linearly dependent on the applied voltage, in S_1, S_2, S_4, and S_5 samples. In real semiconductors, these leakage currents are simply realized by the recombination of the excited charge carriers. These leakage currents are typically caused by defects or other deviations from the ideal semiconductor structure which gives rise to the appearance of allowed energy levels within the bandgap [18]. Also, the observed leakage current may be attributed to Al penetration into the organic film during the deposition of the Al cathode. Deep penetration of Al atoms and their movement towards the other electrode would increase the leakage current and reduce the brightness of the device, as charge recombination would be less likely [19, 20]. It is clear from Fig. 4 that the leakage current in S_3 is too small compared with the leakage currents in the other samples. This may be attributed to an ideal semiconductor structure i.e. no allowed energy levels within the bandgap are formed [18].

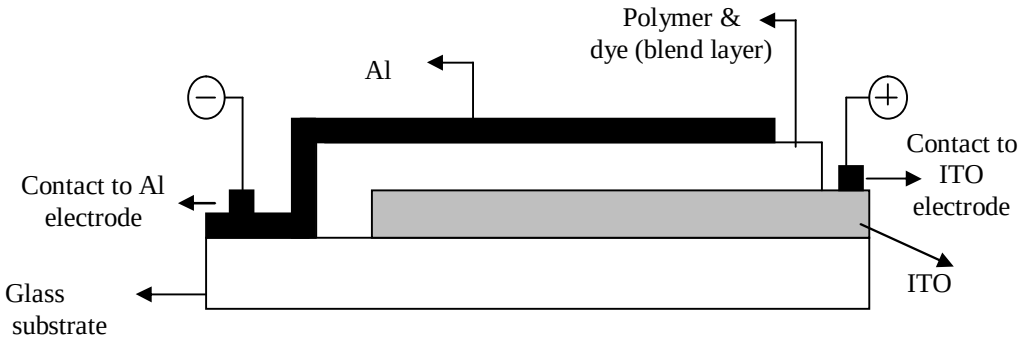

(a)

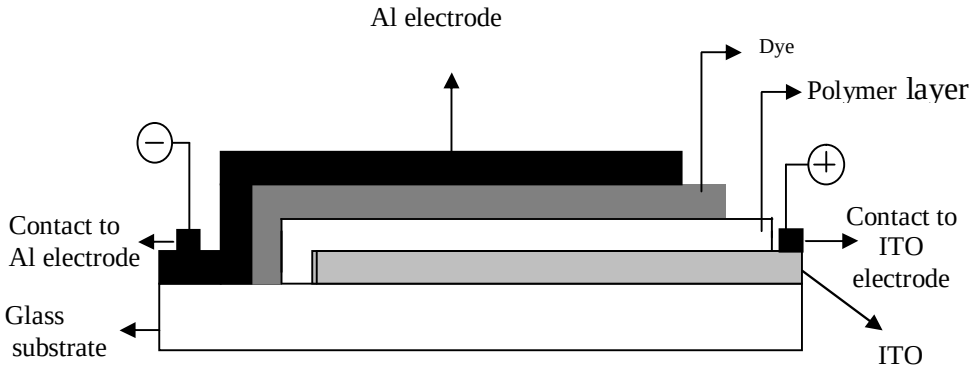

(b)

Fig. 2. Typical structure of (a) a single layer OLED sample, and (b) a double layer OLED sample.

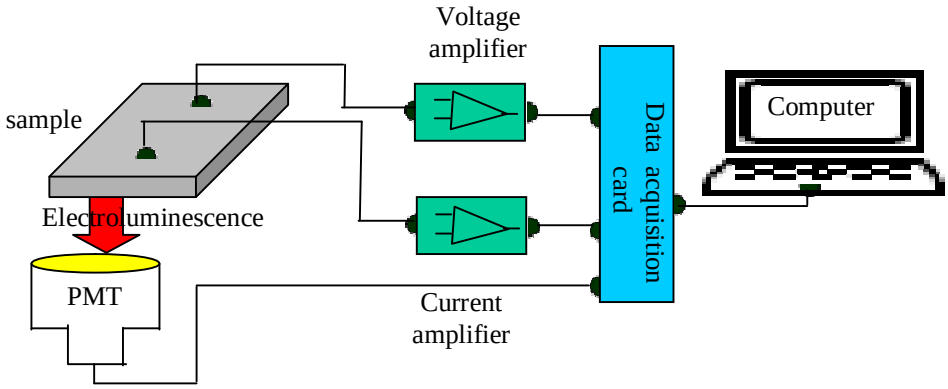

Fig. 3. A schematic diagram of the experimental setup.

Figures 5 through 9 show the dependence of the current I on the voltage V in natural logarithmic scale. Three (or four) regions can be seen in these curves. Curves of S_1 and S_3 can be divided into three regions (marked AB, BC, and CD) whereas curves of S_2, S_4 and S_5 can be divided into four regions (marked AB, BC, CD, and DE).

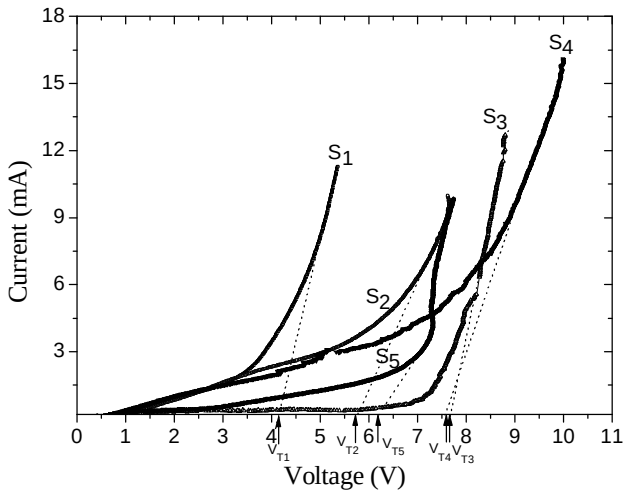

Fig. 4. I-V characteristics for each sample.

Table I: The structure and the threshold voltage V_T for each sample.

Sample	Sample structure	Threshold voltage (V)
S_1	ITO/PVK+R6G (blend)/Al	V_{T1} ~ 4.2
S_2	ITO/PVK / Alq_3 /Al	V_{T2} ~ 5.7
S_3	ITO/PVK +carbocyanine(blend)/Al	V_{T3} ~ 7.7
S_4	ITO/PVK +1,2,4 oxadiazole(blend)/Al	V_{T4} ~ 7.6
S_5	ITO/PVK+fluroscein (blend)/Al	V_{T5} ~ 6.2

These different regions have different slopes and hence different conduction mechanisms. Ohmic conduction at low voltage and space charge limited current SCLC at higher voltage can be expected. In the first region (AB), slopes of the curves for all samples are approximately equal unity, indicating that the conduction mechanism is ohmic [21]. This also means that at low voltages the current is linearly proportional to the applied voltage. In this conduction mechanism, the current density J_{ohm} is given by

$$J_{ohm} = nqm_q \frac{V}{d}, \quad (1)$$

where n is the charge density, q is the electronic charge, m_q is the electron mobility, V is the applied voltage, and d is the thickness of polymer layer [22].

Beyond the ohmic region, the dependence of the current on the voltage follows a power law (IaV^m), where m > 1 is the slope of the log-log IV curves. In these regions, the dominant conduction mechanism is space charge limited current (SCLC) [21]. When the slope approaches 2, the current I is quadratically dependent on the voltage V. This behavior is a characteristic for trap-free SCLC mechanism [21] in which the current density is given by Mott-Gurney equation [23]

$$J_{SCLC} = \frac{9}{8} em_q \frac{V^2}{d^3}, \quad (2)$$

where ε is the permittivity.

The conduction mechanism of regions with high slopes can be attributed to trapped SCLC [21]. Such behavior can be found in region CD in S_1 and S_3 and in region DE in S_2, S_4, and S_5.

The values of slopes for all regions of each sample are tabulated in table (2). S_2 has the largest slope in BC-region (~ 1.62), and the smallest slope

appears in S_3 (~ 0.39) for the same region. For other samples, the slope ranges between 0.55 and 1.6 in this region.

In CD-region, the following remarks can be observed. S_5 has the slope (~ 1.73). SCLC can occur in S_5 in this region if at least one electrode (Al or ITO) layer is able to inject more charge carriers than the material has in thermal equilibrium without carrier injection [22] so that the thermally generated charge contribution is negligible. However, the lowest slope in this region was obtained for S_2 (~ 1.08), this means the conduction is ohmic at this region of S_2, but the largest slope is (~ 3.77) for S_3.

In the fourth region (DE), the slopes have high values. In this region, many conduction mechanisms are involved since the preparation steps of the samples were not simultaneous. This causes oxygen and H_2O trapping. Also penetration of Al atoms into the organic polymer and their movement towards the other electrode would affect the conduction process.

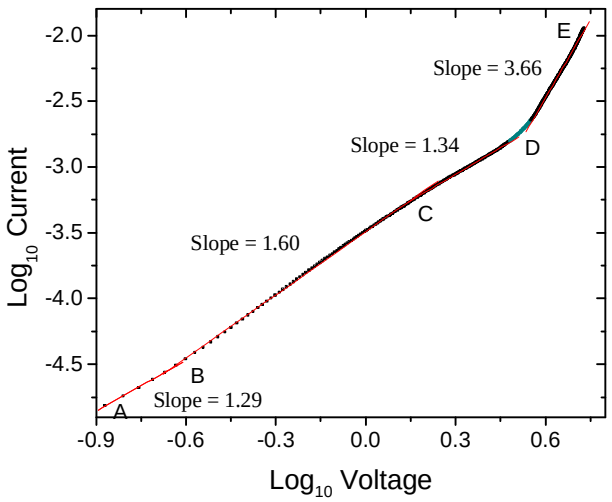

Fig. 5. Current versus voltage in logarithmic scale for sample S_1.

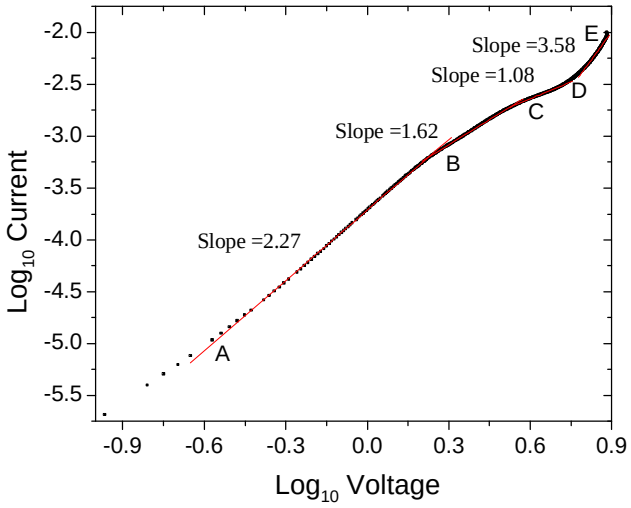

Fig. 6. Current versus voltage in logarithmic scale for sample S_2.

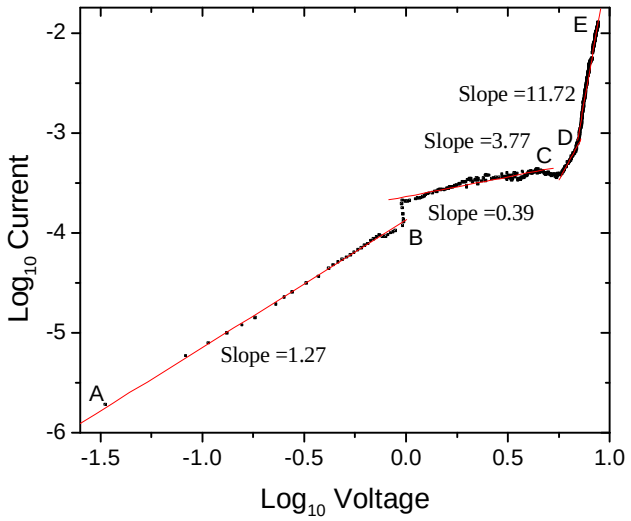

Fig. 7. Current versus voltage in logarithmic scale for sample S_3.

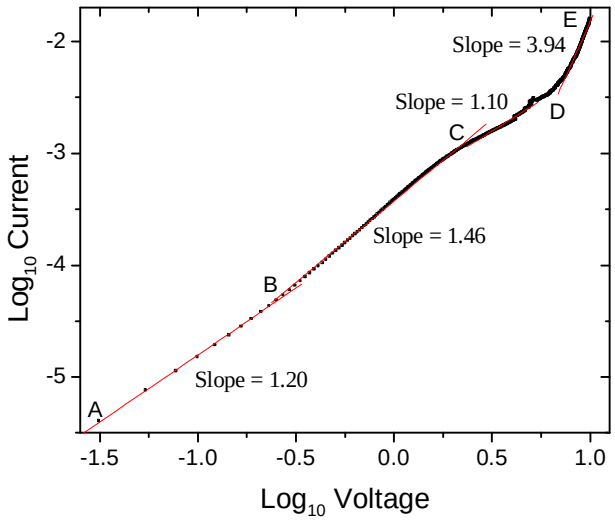

Fig. 8. Current versus voltage in logarithmic scale for sample S_4.

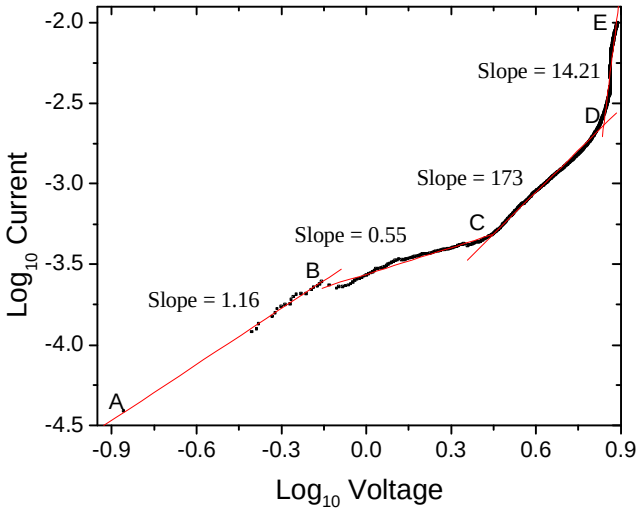

Fig. 9. Current versus voltage in logarithmic scale for sample S_5.

Table II: Approximate values of slope for each region of current-voltage of the five OLED samples in logarithmic scale.

Region	S_1	S_2	S_3	S_4	S_5
AB	1.29	2.27	1.27	1.20	1.16
BC	1.60	1.62	0.39	1.46	0.55
CD	1.34	1.08	3.77	1.10	1.73
DE	3.66	3.58	11.72	3.94	14.21

The variation of the EL of each device with the driving voltage is depicted in Fig. 10. An inset showing the curve of S_2 has been provided in this figure since the curve of S_2 overlaps with part of that of S_4. This figure reveals that the EL increases with increasing the applied voltage. At low voltages no light emission was observed. When the applied voltage exceeds V_T, light emission can be clearly observed by the naked eye in a semi-dark room. The figure reveals that the EL threshold voltage for each sample is almost as given in table (1). The improved performance of S_3 and S_4 over that of other samples is clearly observed in this figure. The reason for this improved performance is probably due to the good balance in the number of injected holes and electrons in the S_3 and S_4 samples compared to other samples.

Figure 11 shows the variation of the EL with current. Almost all samples exhibit a linear dependence of EL on the current [24]. The figure also shows that the largest leakage current occurs in S_2 (~ 5.4 mA). On the other hand, the leakage currents in S_1 and S_5 devices are ~ 3.8 mA and ~ 2.9 mA, respectively.

For all devices, light emission can be clearly observed by the naked eye in a semi-dark room when the bias exceeds V_T. This performance may be enhanced by incorporating an additional electron transport layer as well as buffer layers. Such layers may cause a charge balance in the emitting layer which is necessary to produce a bright and efficient device. Moreover, the recombination zone will be located away from the metal electrode, lowering the probability that the light emission will be quenched by the metallic Al cathode [25].

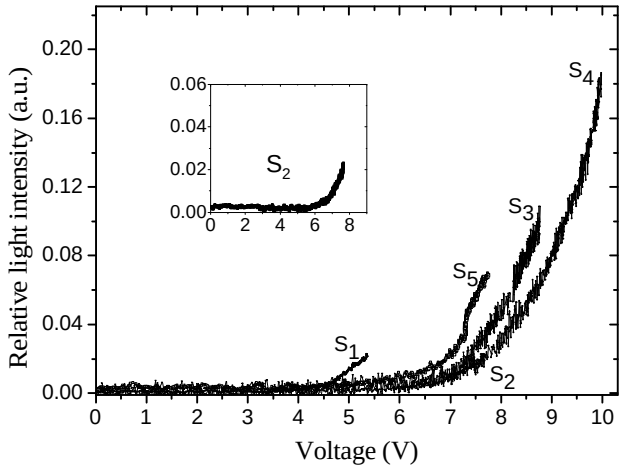

Fig. 10. The relative intensity-voltage curve for all samples.

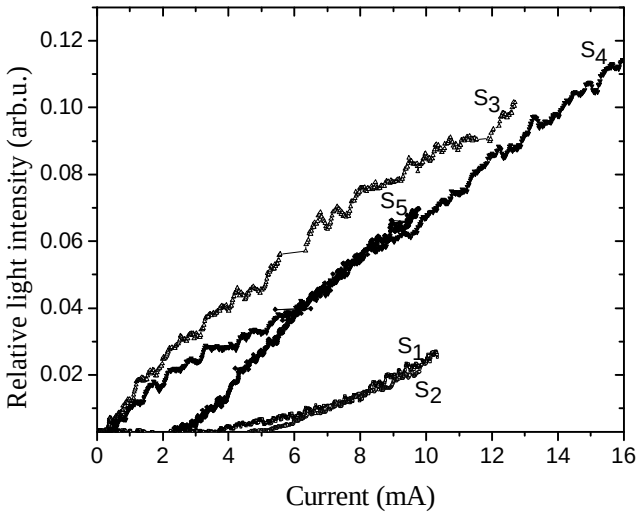

Fig. 11. Relative light intensity versus current for all samples.

Conclusions

We report electroluminescence from devices composed of a single and double PVK layers, doped with new organic compounds. The dopants were Rhodamine 6G, carbocyanine, 12,4 oxadiazole and fluroscein dyes. More work is needed to improve the performance of these devices by varying the dopant concentrations and incorporating additional electron transport layers as well as buffer layers.

References

[1] C. Tang, S. VanSlyke, *Appl. Phys. Lett.* 51, 913 (1987).
[2] J. Burroughes, D. Bradley, A. Brown, R. Marks, K. Mackay, R. Friend, P. Burn, A. Holmes, *Nature* 374, 539 (1990).
[3] J. Blatchford, A. Epstein, *Am. J. Phys.* 64, 120 (1996).
[4] H. Koezuka, A. Tsumura, T. Ando, *Synth. Met.* 18, 699 (1987).
[5] L. Majewski, R. Schroeder, M. Grell, *Appl. Phys. Lett.* 85, 3620 (2004).
[6] C. Tang, *Appl. Phys. Lett.* **48**, 183 (1986).
[7] A. MacDiarmid, R. Kaner, *Electrochemistry of PA: application to rechargeable batteries*, Marcel Dekker, New York, 1986.
[8] D. Braun, A. Heeger, *Appl. Phys. Lett.* 58, 1982 (1991).
[9] J. Kim, S. Noh, K. Kim, S. Lim, D. Shin, Synthetic Metals 117, 227 (2001).
[10] J. Chung, B. Choi, H. Lee, *Appl. Phys. Lett.* 74, 3645 (1999).
[11] U. Mitschke, P. Bäuerle, J. Mater. *Chem.*10, 1471 (2000).
[12] J. M. pearson, (*Vinylcarbazole Polymers*) in Encyclopedia of Polymer Science and Engineering, Wiley, New York, 1989.
[13] Y. Zhang, T. Wada, H. Sasabe, *J. Mater. Chem.* 8, 809 (1998).
[14]
[15] G. Johnson, K. McGrane, M. Stolka, *Pure & Appl. Chem.* 67, 175 (1995).
[16] H. Riel, S. Karg, T. Beierlein, B. Ruhstaller, W. Rie, *Appl. Phys. Lett.* 82, 466 (2003).
[17] X. Zhou, J. Blochwitz, M. Pfeiffer, A. Nollau, T. Fritz, K. Leo, *Adv. Funct. Mater*. 11, 310 (2001).
[18] Klaus Petritsch, *Organic Solar Cell Architectures* , PhD Thesis, Technisch-Naturwissenschaftliche Fakultät der Technischen Universität Graz (Austria), Cambridge and Graz, July 2000.
[19] T. El-Agez, A. El Tayyan, M. Abdel-Latif, *J. of Islamic University of Gaza*, 14, 1 (2006).

[20] M. Stössel, A. Seimens, G. Wittmann, K. Heuser, J. Blässing, M. Inbasekaran, *Proc. SPIE*. 4105, 92 (2001).
[21] K. Kao, *Dielectric phenomena in solids*, Elsevier Academic Press, San Diego, California, 2004.
[22] F. Michelotti, F. Borghese, M. Bertolotti, E. Cianci, V. Foglietti, Alq_3/PVK heterojunction electroluminescent devices, *Synthetic Metals* 111, 105 (2000).
[23] N. F. Mott, R. W. Gurney, *Electronic Processes in Ionic Crystals*, Dover, New York, 1940.
[24] C. Leea, G. Kanga, J. Jeona, *Thin Solid Films* 363, 306 (2000).
[25] A. El Tayyan, T. El-Agez, M. Abdel-Latif, *Chinese J. Phys*. 46, 153 (2008).